The Protein Journal, Vol. 26, No. 1, January 2007 (© 2006)
DOI: 10.1007/s10930-006-9013-8
Published online: November 30, 2006

The Use of the Free Metal – Temperature 'Phase Diagrams' for Studies of Single Site Metal Binding Proteins

Sergei E. Permyakov[1] and Eugene A. Permyakov[1,2]

Typical physico-chemical studies of metal binding proteins are usually aimed at determination of the metal binding constant K for a native protein (K_n), while the significance of the K value for the thermally denatured protein (K_u) is usually underestimated. Meanwhile, metal binding induced shift of thermal denaturation transition of a single site metal binding protein is defined by K_n to K_u ratio, implying that knowledge of both K values is required for full characterization of the system. In the present work, the most universal approach to the studies of single site metal binding proteins, namely construction of a protein ''phase diagram'' in coordinates of free metal ion concentration – temperature, is considered in detail. The detailed algorithm of construction of the phase diagrams along with underlying mathematic procedures developed here may be of use for studies of other simple protein-target type systems, where target represents low molecular weight ligand. Analysis of the simplest protein-ligand system reveals that thermodynamic properties of apo-protein dictate the maximal possible increase of its affinity to any simple ligand upon thermal denaturation of the protein. Experimental and general problems coupled with the use of the phase diagrams are discussed.

KEY WORDS: ligand binding; metal binding; phase transition; stability; thermodynamics.

1. INTRODUCTION

Metal binding proteins play numerous important roles in various vital biological processes. Some of intracellular metal binding proteins serve as metal dependent switches of regulatory pathways, others modulate metal ions flows inside cells. The pivotal roles of calcium modulated proteins located inside cells, in the cell membranes and outside cells are well established (reviewed, for example, by (Berchtold *et al.*, 2000; Carafoli, 2002; Clapham, 1995; Haeseleer *et al.*, 2002; Persechini *et al.*, 1989)). Among a wide variety of eukaryotic cells, ranging from fungi to mammals, Ca^{2+} ion serves as a universal messenger, transmitting signals from the cell surface to the interior of the cell. Depending on the signal and cell type, cytosolic free Ca^{2+} can be increased by an influx of external calcium *via* calcium channels or a calcium release from intracellular stores. Changes in free calcium concentration have been associated with the regulation of a wide variety of cellular processes as important and disparate as cell differentiation, transport, motility, gene expression, stress signals (cold and heat shock), metabolism, cell cycle and pathogenesis. Although a similar role for this divalent cation in prokaryotes is still elusive, there is increasing interest and evidence for calcium as a regulator in bacteria (reviewed by (Dominguez, 2004)). Like eukaryotes, bacterial cells have ion channels, primary and secondary transporters, and calcium binding proteins, which may be involved in Ca^{2+} homeostasis. While magnesium and monovalent cations, sodium and potassium,

[1] Institute for Biological Instrumentation of the Russian Academy of Sciences, Pushchino, Moscow region, 142290, Russia
[2] To whom correspondence should be addressed. E-mail: permyakov@ibp-ran.ru

compete for most of the calcium binding sites, the whole set of divalent cations, like zinc, copper, manganese and others, were shown to bind to other sites, distinct from the calcium binding sites. Physiological significance of zinc binding proteins was corroborated in multiple studies (for reviews, see (Chai *et al*., 1999; Laity *et al*., 2001; Matthews and Sunde, 2002; Ugarte and Osborne, 2001)). Cells avidly acquire a variety of transition elements and ultimately employ them in structurally constrained binding sites, where they can carry out regulatory or catalytic roles. Zinc is essential for cell proliferation and differentiation, especially for the regulation of DNA synthesis and mitosis (reviewed by Beyersmann and Haase (2001)). It can modulate cellular signal recognition, second messenger metabolism, protein kinase and protein phosphatase activities, and it may stimulate or inhibit activities of transcription factors. Zinc ions were shown to be indispensable for brain, olfactory (reviewed by Takeda (2001)) and visual functions (Ugarte and Osborne, 2001). The structural features of the metal ion binding sites have been studied in detail (for reviews, see Chakrabarti (1990), Auld (2001), Krishna *et al*., (2003)). The results of extensive physico-chemical studies of metal binding proteins demonstrate that typically their physico-chemical properties strongly depend upon the binding of metal cations, which seems to explain the versatility of functions performed by metal binding proteins in living organisms. For this reason, characterization of the metal-induced changes of key thermodynamic properties of metal binding proteins represents highly actual task of modern molecular biophysics.

It is well known that the apparent affinity of a protein for Ca^{2+} strongly depends upon temperature and concentrations of competing cations (Mg^{2+}, Na^{+} and K^{+}) and other agents, which are able to interact with the protein. Even in the absence of any other components in solution, except for the protein and Ca^{2+} ions, the full-scale characterization of protein calcium binding properties is a challenging task. Even for the simplest one-site calcium binding protein possessing a single thermal transition, calcium affinity for at least two protein states, native and thermally denatured (unfolded) ones, should be characterized. However, the general practice in characterization of metal binding proteins is to measure only the metal affinity of the native protein; even though, the relationship between metal affinities for native and unfolded protein states and metal induced thermal stability changes is well known. The situation may be additionally complicated since some metal binding proteins in the absence of bound cations unfold at fairly low temperatures, often at room temperatures or even lower (for example, α-lactalbumin (Dolgikh *et al*., 1981; Permyakov *et al*., 1985) and parvalbumin (Filimonov *et al*., 1978; Permyakov *et al*., 1982, 1983)). In this case the measurement of metal binding at room temperatures gives only apparent metal binding constants and involves at least one intermediate state in the course of the measurements. Thus, the measurements of metal binding constants at a single fixed temperature may lead to erroneous conclusions. In order to correctly characterize this system one should study metal binding at different temperatures, measure thermal unfolding of the protein in the presence of various metal concentrations and, finally, to construct a ''phase diagram'' in terms of free metal concentration and temperature.

Strictly speaking, the metal binding-induced structural transition in a protein or its thermal transition can not be considered as a classical phase transition, since certain distinctive features of phase transitions considered in classical physics, like the presence of phase boundary, are absent in this case. Here, the term ''phase transition'' is applied to intramolecular transitions occurring within a protein molecule in response to metal association/dissociation or change of temperature. Nevertheless, the ''phase diagram'' in this case represents the most general and most descriptive characteristic of the protein-metal system, allowing visualization of the regions of predominance of different protein states and prediction of protein states in certain experimental conditions with ease.

The construction of the phase diagram can be performed relatively easily for proteins possessing a single metal binding site, having a single thermal denaturation transition. The diagram of this kind was reported 20 years ago for bovine α-lactalbumin (Permyakov *et al*., 1985), which contains a single high affinity calcium binding site (reviewed in Permyakov (2005)). The fact, that the plotting of phase diagrams in protein systems of this kind did not become a common practice, suggests that mathematical part of this process is generally considered by researches as undesirably complicated. Thus, an additional algorithmization of this procedure, promoting popularization of phase diagrams, is required. Here we present the step-by-step algorithm of construction of phase diagrams for

protein-metal cation systems along with straightforward mathematical procedures underlying this process, which can be successfully used for characterization of other systems of protein-target type, where the target represents some low molecular weight compound. The exemplification of all aspects described here is presented in a separate paper, dedicated to studies of temperature and calcium-binding induced transitions in lysozyme from equine milk (Permyakov *et al*., 2006).

2. RESULTS AND DISCUSSION

2.1. Definitions and Necessary Presumptions

The system under consideration represents some imaginary equilibrium water protein-metal system, maintained at a constant pressure and optimal pH value, distant from pH transitions of all possible forms of the protein, meeting the following requirements:

(1) The protein should possess a single metal binding site, regardless of temperature conditions.
(2) It should possess a single thermal transition, regardless of metal content.
(3) Both native and denatured states of the protein are to be monomeric.
(4) All transitions occurring in the system are to be reversible.

Thus, the system can be represented by the following *four states equilibrium scheme*:

$$\begin{array}{ccccc} & & \alpha(T) & & \\ & \mathrm{N} & \leftrightarrow & \mathrm{D} & \\ & + & & + & \\ & \mathrm{M} & & \mathrm{M} & \\ K_{\mathrm{n}}(T) & \updownarrow & & \updownarrow & K_{\mathrm{u}}(T) \\ & \mathrm{NM} & \leftrightarrow & \mathrm{DM} & \\ & & \beta(T) & & \end{array} \qquad ([1])$$

Here, upper horizontal equilibrium of the four states scheme describes thermal denaturation of the apo-protein (conversion of the native "N" state into denatured "D" state), while lower horizontal equilibrium corresponds to the denaturation of the metal-bound protein form (conversion of the metal-loaded native "NM" state into metal-loaded denatured "DM" state). Two vertical equilibria describe the binding of metal ion "M" to native or denatured states of the protein, respectively.

Apparently, real protein-metal systems may satisfy these requirements to a various extent. The presence of oligomerization/aggregational processes, temperature or pH-induced fragmentation of the protein, availability of additional low-affinity metal binding sites or extra thermal transitions are the factors impeding consideration of real systems. Moreover, in certain systems kinetic limitations may prevent from successful experimental measurements of thermal and metal-induced transitions in the protein. If affinity of native or denatured protein to metal ions exceeds $10^{10}\ M^{-1}$ (some of the zinc finger motifs are characterized by even higher binding constants, see (Mely *et al*., 1996) for example), than, if the metal association kinetics is governed by diffusion process (association rate constant $\sim 10^{8}\ M^{-1}\ s^{-1}$), the dissociation process will require at least 100 s for equilibration. In extreme case, the low rate of exchange between apo- and metal-loaded protein states may result in splitting of the single thermal transition observed experimentally into two separate transitions corresponding to the thermal denaturation of these states. Thus, special precautions are to be taken for adequate experimental determination of the transitions occurring in the system in this case. Hereinafter, we will suppose that experimental data are not affected by any kinetic limitations.

It should be emphasized that the thermally denatured protein may represent both fully unfolded polypeptide chain (random coil-like structure) and a molten globule-like state, characterized by fluctuating tertiary structure and partially conserved secondary structure. The last situation is more complicated since this state can change the content of its residual secondary structure with temperature, although within the framework of the Scheme [1] it is considered as a stable, temperature-independent state. This contradiction can be partially overcome if we take into account enthalpy of metal binding to the denatured protein state.

One more assumption, which is quite conventional, is that activity coefficients of different protein states are very close to each other, so the processes represented by the scheme [1] can be characterized by equilibrium constants, written in the following way ([M] denotes activity of a metal ion):

$$\alpha = [\mathrm{D}]/[\mathrm{N}] \qquad (1)$$

$$\beta = [DM]/[NM] \quad (2)$$

$$K_n = [NM]/([N] \cdot [M]) \quad (3)$$

$$K_u = [DM]/([D] \cdot [M]) \quad (4)$$

A phase diagram is intended for graphical representation of populations of different system states under different environmental conditions. Opposite to macroscopic thermodynamic systems considered in classical physics, where different phases may coexist only on phase separation lines, macromolecular systems are characterized by existence of the vast areas of phase diagrams, where different system states coexist with each other. Exhaustive planar representation of populations of coexistent system states is quite difficult, which gives raise to appearance of multiple possible representation forms of the phase diagrams. The representation described in Rosgen and Hinz (2003) is based upon ''phase separation line'', which is defined by the points in a phase diagram where one state has a population value of 50%. The phase separation lines corresponding to all states of a system divide a phase space into regions of more than 50% population of a separate system state, and the ''n-tupple areas'', defined as regions in the phase diagram where all of the n populated states have a population size smaller than 50%. This representation shares some common features with the phase diagrams described in classical physics, but we believe that a more convenient and general way of presentation of the phase diagrams can be developed for macromolecules.

The most general representation of macromolecular phase diagram would be a three dimensional diagram, describing relative populations of separate macromolecule states in the whole phase space. For planar representation of the phase diagrams we propose to use two different sets of lines. Two primary lines in the phase diagram consist of the points corresponding to the middle of apparent transition in the scale of one of the parameters (for example, temperature or free metal concentration). For each of the system states a set of isolines can be plotted, corresponding to the points in a phase diagram with a fixed relative population (h) of chosen system state. Use of $h = 90\%$ or 99% is highly convenient for evaluation of the regions of the phase space where complete predominance of one of the macromolecule states is observed. Using $h = 50\%$, the abovementioned phase separation lines can be obtained. Consequently, the proposed representation of macromolecular phase diagrams enable both to determine the positions of apparent transitions under conditions of fixed value of one of the parameters and to find the areas of predominance of one system state over the rest, thus fully covering the representation used in Rosgen and Hinz (2003).

2.2. Construction of the Phase Diagram for the Chemical Equilibrium [1]

The four states equilibrium scheme [1] is described by four parameters, defined by Eqs. (1)–(4): α, β, K_n and K_u. Combining these equations, the following relationship between the parameters can be derived:

$$K_u \cdot \alpha = K_n \cdot \beta \quad (5)$$

Consequently, any combination of three of the above-mentioned parameters is suitable for complete description of the system. The remaining fourth parameter can be calculated from the known three parameters from the Eq. (5). Evidently, the phase diagram itself is invariant with respect to the choice of specific set of the parameters, which makes it especially attractive.

The choice of the most convenient for experimental determination triplet of the parameters is dictated by the relative proportion of these parameters. The most representative situations encountered in practice will be considered later in detail. Meanwhile, we will assume that α, K_n and K_u triplet is experimentally determined and will use it for the construction of the phase diagram.

The crucial factor for the adequate description of the Scheme [1] is the accuracy of experimental determination of $\alpha(T)$ (or $\beta(T)$) function. One of the most suitable technique for this purpose is scanning microcalorimetry, which allows getting direct information on enthalpy of thermal denaturation, that gives exhaustive thermodynamic description of the system. Assuming that the difference between heat capacities of the denatured and native protein states (ΔC_p) is independent of temperature, the equilibrium thermal denaturation constant for the two-state transition can be calculated from the van't Hoff's equation:

$$K_t(T) = \exp\left[\frac{\Delta H_{\mathrm{VH}} - \Delta C_p \cdot T_0}{R}\left(\frac{1}{T_0} - \frac{1}{T}\right) + \frac{\Delta C_p}{R}\ln\frac{T}{T_0}\right] \quad (6)$$

Here, ΔH_{VH} is van't Hoff's enthalpy of protein denaturation and T_0 is a mid-transition temperature.

Similarly, the van't Hoff's equation can be used to take into account temperature dependencies of the K_{n} and K_{u} parameters (compare to Eq. (6), assuming that ΔC_p is zero):

$$K_{\mathrm{m}}(T) = K_{\mathrm{m}}(T_0) \cdot \exp[\Delta H \cdot (1/T_0 - 1/T)/R] \quad (7)$$

Here, T_0 is an arbitrarily chosen temperature and ΔH is enthalpy of metal binding, which can be determined directly from isothermal titration calorimetry measurements.

Evidently, the metal binding constant, measured experimentally at a fixed temperature, is in fact an *apparent binding constant*:

$$K_{\mathrm{m}}(T) = ([\mathrm{NM}] + [\mathrm{DM}])/\{([\mathrm{N}] + [\mathrm{D}]) \cdot [\mathrm{M}]\} \quad (8)$$

Combining the Eqs. (1)–(5), the following relationship can be easily obtained:

$$K_{\mathrm{m}}(T) = (K_{\mathrm{u}} \cdot \alpha + K_{\mathrm{n}})/(\alpha + 1) \quad (9)$$

At the middle of the transition, where $K_{\mathrm{m}}(T) = 1/[\mathrm{M}]$,

$$[\mathrm{M}] = (\alpha + 1)/(K_{\mathrm{n}} + \alpha \cdot K_{\mathrm{u}}) \quad (10)$$

The last equation represents the free metal concentration [M] at which the protein is half-loaded with metal ions at a fixed temperature T. The temperature dependence of [M] is the first major curve of the phase diagram (curve 1, see Fig. 1). According to the Eq. (10), it will have two asymptotes, $[\mathrm{M}] = 1/K_{\mathrm{n}}$ (if $\alpha(T) \to 0$) and $[\mathrm{M}] = 1/K_{\mathrm{u}}$ (if $\alpha(T) \to +\infty$), which correspond to the half-transition metal concentrations for metal-induced transitions between native and denatured protein states, respectively (see Fig. 1). Thus, the curve 1 of the phase diagram allows estimation of the K_{n} and K_{u} values with ease.

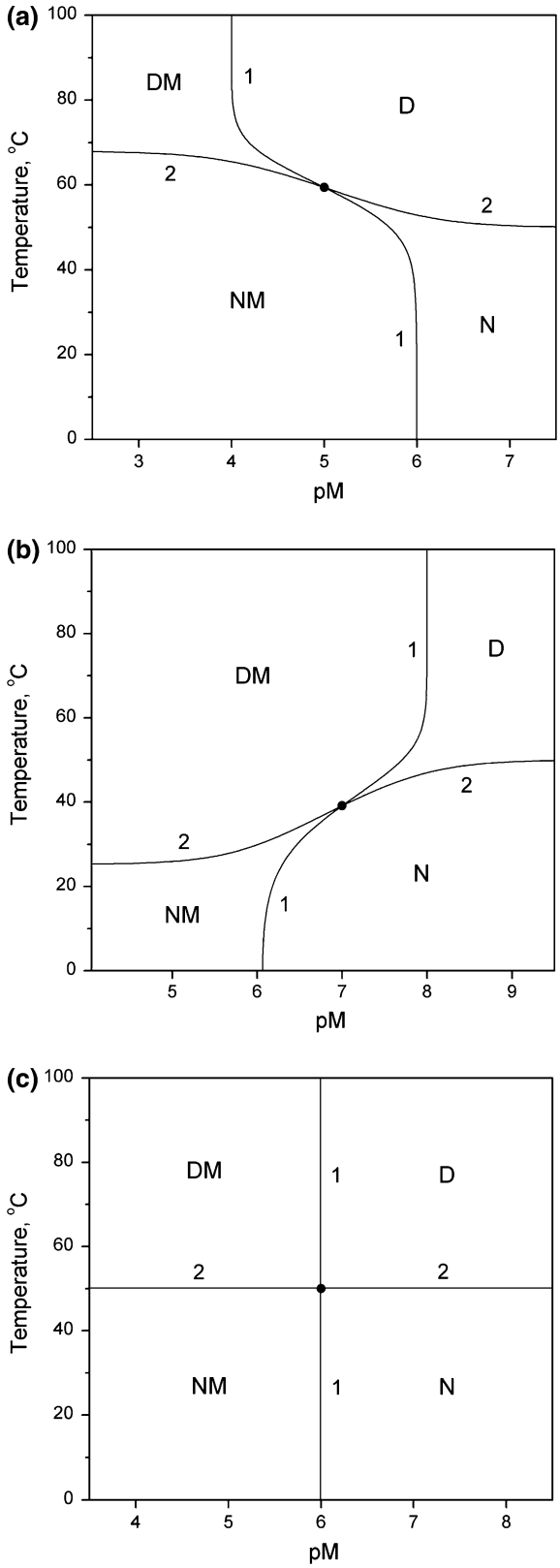

Fig. 1. The dependence of the phase diagram describing the *four states equilibrium scheme* [1] upon K_{n} to K_{u} ratio. $K_{\mathrm{n}} = 10^6$ $1/M$, while K_{u} equals to $K_{\mathrm{n}}/100$ (a), $K_{\mathrm{n}}{\cdot}100$ (b) or K_{n} (c). The thermal transition between the apo-forms of a protein is described by the thermodynamic parameters indicated in Table 1. Curves 1 and 2 correspond to half-transition for binding of metal (Eq. (10)) and thermal denaturation (Eq. (13)), respectively.

The *apparent equilibrium constant for conversion of the native protein to the thermally denatured state* is

$$K_t(T) = ([D] + [DM])/([N] + [NM]) \quad (11)$$

Taking into consideration Eqs. (1)–(4), K_t can be rewritten as

$$K_t(T) = \alpha \cdot (1 + K_u \cdot [M])/(1 + K_n \cdot [M]) \quad (12)$$

Consequently, at mid-transition temperature ($T_{1/2}$), where $K_t(T_{1/2}) = 1$, the following condition takes place:

$$[M] = (\alpha - 1)/(K_n - \alpha \cdot K_u) \quad (13)$$

The last equation defines the second primary curve of the phase diagram (curve 2), giving the position of the thermal denaturation transition as a function of free metal concentration. Apparently, the last equation is valid only if $K_n \neq K_u$, otherwise, according to Eq. (12), $T_{1/2}$ is independent of metal concentration. According to the Eq. (13), the curve 2 will possess two asymptotes: T values, at which $\alpha(T) = 1$ or $\alpha(T) = K_n/K_u = \alpha(T)/\beta(T)$ (see Eq. (5)), which is equivalent to $\beta(T) = 1$ (see Fig. 1). Thus, the curve 2 of the phase diagram allows evaluation of the mid-transition temperatures of the thermal denaturation transitions between apo- and metal-loaded protein states.

Importantly, based upon the asymptotic values one can conclude that the more the difference between K_n and K_u values, the more pronounced thermal stability shift is observed in response to the metal binding. This well known conclusion is related to the fact that the differences in K_n and K_u values are actually related to protein energetics. As follows from the four states Scheme [1], the difference ($\delta\Delta G$) between the free energies of denaturation of metal-saturated (ΔG_{Me}) and apo- (ΔG_{apo}) protein forms equals to the difference in the free energies of the metal-binding for denatured and native protein states, which leads to the equation:

$$\delta\Delta G = \Delta G_{Me} - \Delta G_{apo} = RT \cdot \ln(K_n/K_u) \quad (14)$$

It means that the metal-induced change in protein thermal stability depends upon the K_n to K_u ratio: if thermal denaturation lowers protein affinity to metal ions ($K_n > K_u$), then metal association is accompanied with an increase in thermal stability ($\delta\Delta G > 0$), and *vice versa*.

The dependence of the metal binding induced thermal transition shift upon K_u/K_n ratio can be obtained as follows. According to the Eqs. (5) and (6), in the middle of the thermal transition between the metal-bound forms of a protein, we have the relationship:

$$\ln(K_u/K_n) = \ln(\beta/\alpha) = \frac{\Delta H_{VH} - \Delta C_p \cdot T_{1/2,\alpha}}{R}\left(\frac{1}{T_{1/2,\beta}} - \frac{1}{T_{1/2,\alpha}}\right) - \frac{\Delta C_p}{R}\ln\frac{T_{1/2,\beta}}{T_{1/2,\alpha}} \quad (15)$$

Here, $T_{1/2,\beta}$ and $T_{1/2,\alpha}$ are the mid-transition temperatures, corresponding to the thermal transitions described by the equilibrium constants β and α, respectively. Assuming that the thermal transition between the apo-forms of a protein is described by the thermodynamic parameters indicated in Table 1, the dependence of the metal binding induced thermal transition shift ($T_{1/2,\beta} - T_{1/2,\alpha}$) upon $\lg(K_u/K_n)$ will look as shown in Fig. 2. The decrease in the K_u to K_n ratio below 1 is accompanied with nearly constant increase of the thermal transition shift. On the contrary, the sharp decrease in the thermal transition shift upon the increase of the K_u to K_n ratio occurs when we approach to the temperature, at which the maximum excess of native apo-protein upon denatured is reached. Importantly, this conclusion is independent of the model, used for approximation of the $\alpha(T)$ function. Thus, knowing only parameters of the thermal denaturation of the apo-protein one can predict the maximal K_u/K_n ratio ever possible for any substance which is able to associate with the protein according to the Scheme [1]. According to the Eq. (15), the maximal possible K_u/K_n ratio equals to the reversed minimum $\alpha(T)$ value, which is equivalent to the maximal value of $\exp[\Delta G(T)/(RT)]$ function, where $\Delta G(T)$ is the free energy change upon denaturation of apo-protein. Thus, thermodynamic properties of apo-protein dictate the maximal possible increase of its affinity for any simple ligand upon thermal denaturation of the protein.

Table 1. The Thermodynamic Parameters of the Model Two-state Thermal Transition of a Protein

T_0, °C	ΔH_{VH}, kJ/mol	ΔC_p, kJ/(mol K)
50	200	4

T_0 is a mid-transition temperature, ΔH_{VH} is van't Hoff's enthalpy of protein denaturation and ΔC_p is the difference between heat capacities of the denatured and native protein states, respectively.

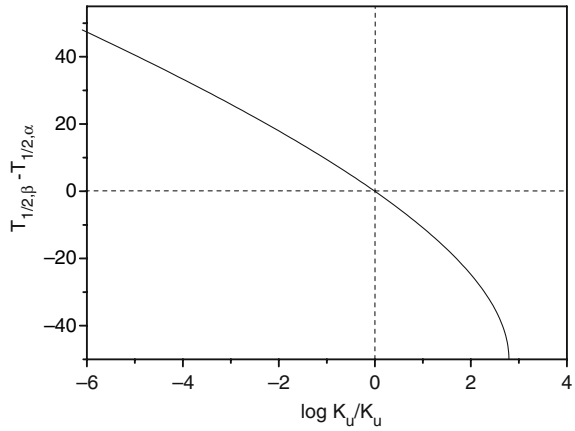

Fig. 2. The dependence of the thermal transition shift ($T_{1/2,\beta} - T_{1/2,\alpha}$) induced by metal binding upon K_u to K_n ratio, calculated according to the Eq. (15), assuming that the thermal transition between the apo-forms of a protein is described by the thermodynamic parameters indicated in Table 1.

The intersection of the curves 1 and 2 can be determined by solving the system of Eqs. (10) and (13), which gives the following solution:

$$-\lg[\mathrm{M}] = \lg(K_\mathrm{n} \cdot K_\mathrm{u})/2 \tag{16}$$

The two protein states [N] and [DM] are present in equal concentrations in this point, as well as the two other forms [NM] and [D]. The relative population of these states depends upon the K_n to K_u ratio:

$$[\mathrm{N}] = 0.5 \cdot \mathrm{P}_0/[1 + (K_\mathrm{n}/K_\mathrm{u})^{1/2}] \tag{17}$$

Here, P_0 is the total protein concentration in the system.

The foregoing consideration of the four states equilibrium Scheme [1] demonstrates that the key characteristics of the phase diagram are dictated by the K_n to K_u values ratio. Figure 1 shows frames of the phase diagrams calculated for different K_n to K_u ratios. The curves 1 and 2 divide the free metal concentration – temperature space into four regions roughly corresponding to the areas of predominance of different protein states ([N], [NM], [D] and [DM]).

To complete the phase diagram a set of isolines should be plotted. The isolines corresponding to the points in a phase diagram with a fixed excess of one protein form over the others may be plotted in the following manner. The system of equations, describing the isolines of the phase diagram, includes: Eqs. (1), (3), (4)

$$[\mathrm{X}] = h \cdot P_0, h<1 \tag{18}$$

$$[\mathrm{N}] + [\mathrm{NM}] + [\mathrm{D}] + [\mathrm{DM}] = P_0 \tag{19}$$

Here, [X] corresponds to any of the possible protein states and h is a coefficient, determining the excess of the protein form of interest over the other forms. Solving the system, we will get the following expressions for free metal concentration [M] (note, that the results are independent of protein concentration P_0):

$$1)[\mathrm{X}] \equiv [\mathrm{N}] : [\mathrm{M}] = (1/h - 1 - \alpha)/(K_\mathrm{n} + \alpha \cdot K_\mathrm{u}) \tag{20}$$

$$2)[\mathrm{X}] \equiv [\mathrm{NM}] : [\mathrm{M}] = (\alpha + 1)/[K_\mathrm{n} \cdot (1/h - 1) - \alpha \cdot K_\mathrm{u}] \tag{21}$$

$$3)[\mathrm{X}] \equiv [\mathrm{D}] : [\mathrm{M}] = [\alpha \cdot (1/h - 1) - 1]/(K_\mathrm{n} + \alpha \cdot K_\mathrm{u}) \tag{22}$$

$$4)[\mathrm{X}] \equiv [\mathrm{DM}] : [\mathrm{M}] = (\alpha + 1)/[\alpha \cdot (1/h - 1) \cdot K_\mathrm{u} - K_\mathrm{n}] \tag{23}$$

The use of $h = 0.5$ will produce the phase separation lines, described in Rosgen and Hinz (2003). We believe that the use of h values 0.9 or 0.99 is much more convenient for evaluation of the regions of the phase space where complete predominance of one of the protein states is achieved. The complete phase diagram plotted for a model protein using $h = 0.9$ or 0.99 is shown in Fig. 3. Knowing current temperature and $p\mathrm{M} = -\log[\mathrm{M}]$ values, the actual protein state can be assessed. Adding the h parameter as an additional dimension of the diagram, a three-dimensional phase diagram may be plotted. The diagram contains the exhaustive information on population of different protein states for each point of the phase space. Meanwhile, the three-dimensional diagram looses the clearness and the simplicity of handling.

Evidently, the region of the phase diagram with pM values below 1–2 should be treated with great cautious, since ionic strength, which was not taken into account in our calculations, may come into play here. Moreover, saturation of the secondary low affinity metal binding sites of a protein may cause extra deviations of the real protein behavior from that predicted by the phase diagram. In this sense the phase diagram enables one to gain information about the system which is inaccessible in direct measurements.

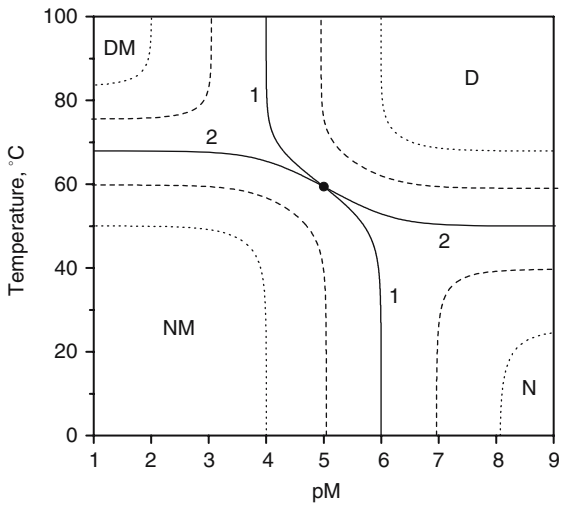

Fig. 3. Phase diagram of a model protein in the free metal concentration – temperature space, calculated according to the *four-states scheme* [1]. The thermal transition between the apo-forms of a protein is described by the thermodynamic parameters indicated in Table 1. $K_n = 10^6\ 1/M$, $K_u = K_n/100$. Curves 1 and 2 correspond to half-transition for binding of metal and thermal denaturation, respectively. The isolines, corresponding to a fixed excess of one protein form over the others, h, are calculated using $h = 0.90$ (dashed line) and $h = 0.99$ (dotted line) according to the Eqs. (20)–(23).

2.3. Experimental Determination of the Parameters of the Equilibrium Scheme [1]

Although the construction of the phase diagram corresponding to the four states scheme of chemical equilibria [1] is very simple and straightforward, the task of experimental evaluation of its parameters (α, β, K_n and K_u) may be quite complicated, depending upon the relationship between the key parameters determining the behavior of the system, K_n and K_u. Here we will consider the most representative situations encountered in practice, in which simple and efficient estimation of the parameters of the scheme [1] is possible. In any case the algorithm of the process looks as follows:

(1) The choice of the major parameter, which should be measured first and will be used for determination of the remaining parameters of the system.
(2) The estimation of the second parameter, based upon the known major parameter.
(3) The estimation of the third parameter, based upon the known two other parameters.

The remaining fourth parameter can be calculated from the known three parameters using the Eq. (5).

$K_u \ll K_n$. According to the Eq. (5) or (14), in this case the metal binding to a protein is accompanied with substantial thermal stabilization. The dependence of the metal binding induced thermal transition shift upon the K_u to K_n ratio can be described by Eq. (15) (see Fig. 2). This situation is quite common for high affinity calcium binding proteins. For example, α-lactalbumin (Dolgikh *et al.*, 1981; Permyakov *et al.*, 1985), parvalbumin (Filimonov *et al.*, 1978; Permyakov *et al.*, 1982, 1983) and other members of the EF-hand family of calcium binding proteins demonstrate significant increase in thermal stability upon calcium association.

If K_u value is about $10^3\ M^{-1}$ or lower, the saturation of the protein with metal ion will require millimolar or higher concentrations of the metal, which may result in effects related to ionic strength change and/or manifestation of the secondary low affinity metal binding sites of the protein. For these reasons, in this case the direct measurement of both K_u and β becomes problematic.

In a general case, the metal binding constant, measured experimentally at a fixed temperature, is actually an apparent binding constant. It is described by Eq. (9), demonstrating that both K_u and K_n constants contribute to the experimentally measured metal binding constant. Therefore, experimental determination of K_n requires thorough choice of temperature conditions. Consequently, the only parameter of the system, which can be measured relatively easily, is α. However, the measurement of the thermal denaturation of apo-protein requires to ensure low free metal concentrations not exceeding $1/(10\ K_n)$ in the course of the measurement. This circumstance imply that: (1) some preliminary estimation of K_n value is necessary; (2) in some cases special metal depletion procedures are required, including the use of strong metal chelators. Despite these difficulties we will assume that $\alpha(T)$ dependence can be successfully measured, for example, from differential scanning calorimetry data (see Eq. (6)), and we will use it as a major parameter.

The knowledge of α enables us to find K_n easily. Taking into account that according to the Eq. (5) $K_u \cdot \alpha = K_n \cdot \beta$, upon $\beta \ll 1$ the Eq. (9) can be rewritten as:

$$K_m(T) \approx K_n/(\alpha + 1) \tag{24}$$

Thus, the measurement of an apparent metal binding constant at low enough temperatures, at which the metal-bound protein form is far from the middle of its thermal transition (see Fig. 4a), will allow rigorous evaluation of K_n by fitting the $K_m(T)$ dependence using K_n as a fitting parameter. Moreover, enthalpy of the metal binding can be evaluated according to the Eq. (7), using enthalpy as an additional fitting parameter.

To complete characterization of thermodynamic parameters of the scheme of chemical equilibria [1] it is enough to estimate equilibrium metal binding constant for the denatured state of the protein, K_u. According to the Eq. (13), in the middle of the thermal transition K_u can be determined from the following equation:

$$K_u = \{1 - \alpha(T_{1/2}) + K_n \cdot [M]\}/\{\alpha(T_{1/2}) \cdot [M]\} \quad (25)$$

If the total metal ion concentration M_0 substantially exceeds protein concentration, then the difference between M_0 and the free metal concentration [M] can be neglected. Hence, knowing the value of mid-transition temperature in the presence of known high concentration of metal ion or under conditions of metal buffer controlled free metal concentration, one can easily estimate the value of K_u from Eq. (25) using known $\alpha(T)$ and K_n. Moreover, multiple values of K_u obtained at different free metal concentrations and, respectively, different mid-transition temperatures can be used for evaluation of the enthalpy of metal binding according to the Eq. (7). Figure 4b demonstrates the dependence of mid-transition temperature $T_{1/2}$ upon K_u in the presence of different free metal concentrations for a model system. Importantly, the dependence reaches a limit at a temperature, which can be evaluated from the condition of equality of K_u described by Eq. (25) to zero (K_n·[M] = $\alpha(T_{1/2}) - 1$). Apparently, the higher the [M] value, the higher the temperature T_{limit} at which this condition takes place, which is clearly seen from the Fig. 4b. The larger the difference between T_{limit} and experimentally observed $T_{1/2}$ values, the higher the accuracy of determination of K_u. As follows from the Fig. 4b, the $(T_{limit} - T_{1/2})$ difference increases with the increase of [M]. Meanwhile, determination of very low K_u values (close to 10 M^{-1}) requires too high [M] values, which may cause ionic strength related effects and filling of low affinity metal binding sites.

$K_u \gg K_n$. In this case metal association is accompanied with substantial decrease in protein thermal stability. For example, this situation takes place upon binding of zinc ions to Ca^{2+}-saturated α-lactalbumin (Permyakov *et al.*, 1991).

Similarly to the previous case, if K_n value is about 10^3 M^{-1} or lower, direct measurements of K_n and β will be accompanied with the use of high metal concentrations, which may cause the effects related to ionic strength change and/or filling of the low affinity metal binding sites of the protein. Again, the parameter of the system, most suitable for the role of the major parameter, is α.

Since according to the Eq. (5) $K_n = K_u \cdot \alpha/\beta$, the Eq. (9) upon $\beta \gg 1$ can be rewritten:

$$K_m(T) \approx K_u \cdot \alpha/(\alpha + 1) \quad (26)$$

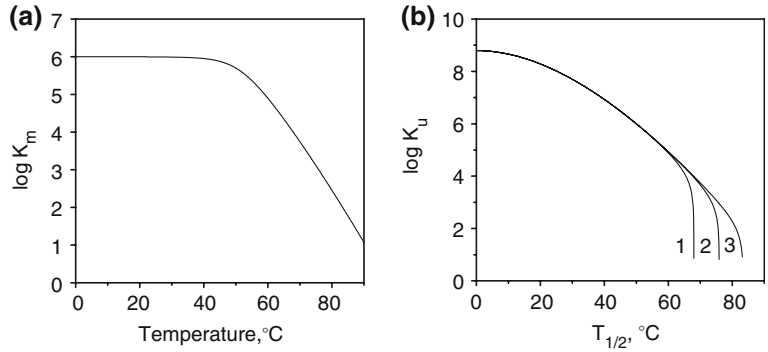

Fig. 4. Experimental determination of the parameters of the *four-states scheme* [1] in the case of $K_u \ll K_n$. The thermal transition between the apo-forms of a protein is described by the thermodynamic parameters indicated in Table 1; $K_n = 10^6$ $1/M$. (a) Temperature dependence of an apparent metal binding constant K_m at temperatures, at which the metal-bound protein form is far from the middle of its thermal transition (see Eq. (24)). (b) Dependence of mid-transition temperature $T_{1/2}$ upon K_u value, in presence of different free metal concentrations: 1, 10^{-4} M; 2, 10^{-3} M; 3, 10^{-2} M (see Eq. (25)).

Hence, the measurement of an apparent metal binding constant at high temperatures, at which the metal-bound protein form is far beyond the middle of its thermal transition (see Fig. 5a), enable one to evaluate K_u by fitting of the $K_m(T)$ dependence using K_u as a fitting parameter.

Analogously, according to the Eq. (13), in the middle of the thermal transition carried out at known free metal concentration,

$$K_n = \alpha(T_{1/2}) \cdot K_u + [\alpha(T_{1/2}) - 1]/[M] \qquad (27)$$

Thus, knowing the value of mid-transition temperature in the presence of known free metal ion concentration, one can easily estimate the value of K_n using known $\alpha(T)$ and K_u. Figure 5b depicts the dependence of mid-transition temperature $T_{1/2}$ upon K_n value in the presence of different free metal concentrations for a model system. Notably, the dependence may reach a limit at certain temperature (curves 1 and 2), which can be obtained from the condition of equality of K_n described by Eq. (27) to zero (K_u·[M] = $1/\alpha(T_{1/2}) - 1$). Apparently, the higher the [M] value, the lower the temperature at which this condition takes place, which is clearly seen from the Fig. 5b. Meanwhile, at [M] values exceeding certain limit this condition will not be fulfilled due to the reaching of the temperature of maximal stability of the protein. This case corresponds to the curve 3 in Fig. 5b.

$K_u \approx K_n$. The difference between thermal stabilities of apo- and metal-bound protein states is minimal in this case.

The situation, when K_u and K_n are about $10^3\ M^{-1}$ or lower is of minor importance, so we will assume that both constants exceed $10^3\ M^{-1}$. In this case both thermal transitions (α and β) may be adequately measured experimentally, without appearance of ionic strength or low-affinity metal-binding related effects. The missing metal binding constant for one of the protein states may be found from Eq. (9), taking into consideration the Eq. (5):

$$K_m(T) = K_n \cdot (\beta + 1)/(\alpha + 1) \qquad (28)$$

So far it was assumed that the major parameter, α, can be measured experimentally. Meanwhile, we should not discard the situation when the mid-transition temperature for apo-protein is close to 0°C or even lower, which makes impossible adequate measurement of α. Apparently, the cases of $K_u \gg K_n$ and $K_u \approx K_n$ upon elevated temperatures are reduced to the two-state scheme in this situation, so only the case of $K_u \ll K_n$ should be considered. Moreover, it will be assumed that K_u value exceeds $10^3\ M^{-1}$, so β(T) can be measured experimentally and used as the major parameter.

According to the Eqs. (5) and (28), if $\alpha \gg 1$, then

$$K_m(T) \approx (\beta + 1) \cdot K_n/\alpha = (\beta + 1) \cdot K_u/\beta \qquad (29)$$

Thus, the measurement of an apparent metal binding constant at high temperatures, at which the apo-protein is far beyond the middle of its thermal transition, allows evaluation of K_u by fitting of the $K_m(T)$ dependence using K_u as a parameter.

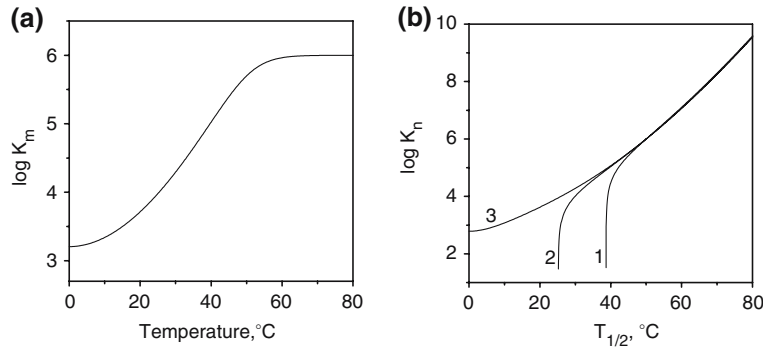

Fig. 5. Experimental determination of the parameters of the *four-states scheme* [1] in the case of $K_u \gg K_n$. The thermal transition between the apo-forms of a protein is described by the thermodynamic parameters indicated in Table 1; $K_u = 10^6\ 1/M$. (a) Temperature dependence of an apparent metal binding constant K_m at temperatures, at which the metal-bound protein form is far beyond the middle of its thermal transition (see Eq. (26)). (b) Dependence of mid-transition temperature $T_{1/2}$ upon K_n value, in presence of different free metal concentrations: 1, $10^{-5}\ M$; 2, $10^{-4}\ M$; 3, $10^{-3}\ M$ (see Eq. (27)).

In the middle of the thermal transition according to the Eq. (13) and taking into account the Eq. (5),

$$K_n = K_u/\{\beta(T_{1/2}) + K_u \cdot [M] \cdot [\beta(T_{1/2}) - 1]\} \quad (30)$$

Thus, knowing the value of the mid-transition temperature in the presence of known free metal concentration, one can easily estimate the value of K_n, based upon known $\beta(T)$ and K_u.

The presented discussion clearly demonstrated the importance of knowledge of the metal binding constant for the thermally denatured protein (K_u) for complete thermodynamic characterization of multiple chemical equilibria occurring in the system. The metal binding induced shift of thermal denaturation transition of a single site metal binding protein is defined by the K_n to K_u ratio (see Eqs. (14) and (15)), implying that knowledge of both values is a must for full characterization of the system. The direct experimental evaluation of the K_u or K_n is likely to be hindered in case of their very low values (below 10^3 M^{-1}) due to the necessity to apply high metal concentrations (above 0.01 M) coupled to the ionic strength change related effects and/or manifestation of the low affinity metal binding sites of the protein. The proposed approach of K_u or K_n estimation in this situation based upon experiments fulfilled at low enough metal concentrations, allows to overcome this complication with ease.

The obtaining of reliable phase diagrams for single site metal binding proteins is coupled to multiple principal problems. The major factors complicating the construction of phase diagrams are:

(1) The necessity to use in certain cases metal chelators for removal of metal ions from protein under study, which sometimes may cause specific interaction between the chelator and the protein, resulting in modification of protein properties. This circumstance implies that additional investigation of chelator binding properties of the protein is to be performed.
(2) If protein thermal denaturation is accompanied with a sharp drop in its affinity for metal ion, then the accuracy of K_u determination may suffer due to the very strong dependence of K_u value upon half-transition temperature (see Fig. 4b). As a result, a small error in experimental $T_{1/2}$ value will produce very high uncertainty in K_u value. The same difficulty takes place for determination of K_n value in the opposite case of significant increase of protein affinity for metal upon thermal denaturation (see Fig. 5b).
(3) The presence of secondary low affinity metal binding site(s) may influence high metal concentration region of the protein phase diagram.
(4) Further increase of metal concentration will inevitably be accompanied with increase of ionic strength of the solution, which was not taken into consideration and may cause an additional distortion of this region of the phase diagram.

Despite the above-mentioned drawbacks of the phase diagrams, their strong features, like generality, clearness, invariability with respect to the choice of specific set of the parameters, suitable for the numerical system description, and the ability to get some protein characteristics which are inaccessible in direct experimental measurements, easily compensate them. Evidently, the same approach can be applied to other two-component systems of protein-target type, where target represents some low molecular substance not subjected to chemical modification upon the interaction. This circumstance substantially extends the domain of applicability of the developed approach. It can be successfully utilized for studies of protein binding of a wide variety of biologically relevant molecules including first and second messengers, macroergic compounds (if the interaction is not accompanied with their chemical modification), vitamins, toxic compounds and many others. The fact, that the practice of plotting of phase diagrams in protein systems of this kind is not a common phenomenon, suggests that mathematical part of this process is generally considered by researches as undesirably complicated. We believe that the step by step algorithm of construction of the phase diagrams as well as underlying mathematic procedures described here will promote popularization of the phase diagrams.

Extension of the principles formulated here to the proteins possessing even two metal binding sites is connected to the necessity to know the exact mechanism of filling of the metal binding sites with ions, which constitute a principal problem by itself. For this reason, the construction of the phase diagram may be highly model-dependent in this case. In this sense the considered case of a single metal binding site represents one of relatively rare systems, which can be characterized my means of phase diagrams without essential conventions.

Although the presented analysis of the *four states equilibrium scheme* [1] was performed

assuming that the transition between native and denatured protein states is induced by temperature change at a constant pressure, the developed mathematical apparatus will be valid also for pressure induced protein denaturation under conditions of constant temperature. Apparently, the Eqs. (6) and (7) should be replaced by their respective analogues in this case. Experimental construction of the phase diagram of this kind is coupled with the necessity to characterize protein affinity for ligand at different pressures in the range of hundreds and thousands of atmospheres, which represents fairly specific technical difficulty. At the same time, the addition of pressure dimension to the phase diagram would allow to gain a full thermodynamic characterization of the protein-ligand system.

ACKNOWLEDGMENT

We are indebted to Prof. R. Kretsinger and Dr. V.N. Uversky for very useful discussion of our work and correction of the manuscript. This work was supported by grants from the Programs of the Russian Academy of Sciences (''Fundamental science for medicine'' and ''Molecular and cellular biology''), Grant 02.442.11.7542 of the Russian Federal Agency for Science and Innovations, Grant 04-04-97322 of the Russian Fund for Basic Research and individual grants to S.E.P. from the ''Russian Science Support Foundation'', RUB2-010001-PU-05 CRDF and the Visby Programme of the Swedish Institute.

REFERENCES

Auld, D. S. (2001) *Biometals* **14:** 271–313.
Berchtold, M. W., Brinkmeier, H., and Muntener, M. (2000). *Physiol. Rev.* **80:** 1215–1265.
Beyersmann, D., and Haase, H. (2001). *Biometals* **14:** 331–341.
Carafoli, E. (2002) *Proc. Natl. Acad. Sci. U. S. A.* **99:** 1115–1122.
Chai, F., Truong-Tran, A. Q., Ho, L. H., and Zalewski, P. D. (1999). *Immunol. Cell Biol.* **77:** 272–278.
Chakrabarti, P. (1990) *Protein Eng.* **4:** 49–56.
Clapham, D. E. (1995) *Cell* **80:** 259–268.
Dolgikh, D. A., Gilmanshin, R. I., Brazhnikov, E. V., Bychkova, V. E., Semisotnov, G. V., Venyaminov, S. Y., and Ptitsyn, O. B. (1981). *FEBS Lett.* **136:** 311–315.
Dominguez, D. C. (2004) *Mol. Microbiol.* **54:** 291–297.
Filimonov, V. V., Pfeil, W., Tsalkova, T. N., and Privalov, P. L. (1978). *Biophys. Chem.* **8:** 117–122.
Haeseleer, F., Imanishi, Y., Sokal, I., Filipek, S., and Palczewski, K. (2002). *Biochem. Biophys. Res. Commun.* **290:** 615–623.
Krishna, S. S., Majumdar, I., and Grishin, N. V. (2003). *Nucleic Acids Res.* **31:** 532–550.
Laity, J. H., Lee, B. M., and Wright, P. E. (2001). *Curr. Opin. Struct. Biol.* **11:** 39–46.
Matthews, J. M., and Sunde, M. (2002). *IUBMB Life* **54:** 351–355.
Mely, Y., De Rocquigny, H., Morellet, N., Roques, B. P., and Gerad, D. (1996). *Biochemistry* **35:** 5175–5182.
Permyakov, E. A. (2005) α-Lactalbumin New York: Nova Science Publishers.
Permyakov, E. A., Medvedkin, V. N., Kalinichenko, L. P., and Burstein, E. A. (1983). *Arch. Biochem. Biophys.* **227:** 9–20.
Permyakov, E. A., Morozova, L. A., and Burstein, E. A. (1985). *Biophys. Chem.* **21:** 21–31.
Permyakov, E. A., Shnyrov, V. L., Kalinichenko, L. P., Kuchar, A., Reyzer, I. L., and Berliner, L. J. (1991). *J. Protein Chem.* **10:** 577–584.
Permyakov, E. A., Yarmolenko, V. V., Burstein, E. A., and Gerday, C. (1982). *Biophys. Chem.* **15:** 19–26.
Permyakov, S. E., Khokhlova, T. I., Nazipova, A. A., Zhadan, A. P., Morozova-Roche, L. A., and Permyakov, E. A. (2006). *Proteins.* **65**: 984–998.
Persechini, A., Moncrief, N. D., and Kretsinger, R. H. (1989). *Trends Neurosci.* **12:** 462–467.
Rosgen, J., and Hinz, H. J. (2003). *J. Mol. Biol.* **328:** 255–271.
Takeda, A. (2001) *Biometals* **14:** 343–351.
Ugarte, M., and Osborne, N. N. (2001). *Prog. Neurobiol.* **64:** 219–249.